SUPPLEMENTARY MATERIALS

Table of Contents

SUPPLEMENTARY MATERIALS AND METHODS

BIOMARKER DISCOVERY p 2
STRUCTURE IDENTIFICATION OF PENTASACCHARIDES p 2
SYNTHESIS OF H3N2b AND d6-H3N2b p 4
CONFIRMATION OF H3N2B STRUCTURE p 6
VALIDATION OF METHODS FOR H3N2b IN HUMAN URINE, PLASMA, AND CSF p 6
REFERENCES p 9

SUPPLEMENTAL FIGURES p 10

SUPPLEMENTAL TABLES p 15

BIOMARKER DISCOVERY

Profiling of ganglioside GM1 in human plasma and CSF samples from GM1 gangliosidosis natural history study

Human plasma, CSF, and urine samples (50 µL) were aliquoted into 2 mL polypropylene tubes (VWR, West Chester, PA). To each tube d_3-GM1(18:0) (400 ng/mL) in methanol (200 µL) was added. The mixtures were vortexed for 3 min and centrifuged for 10 min at 9400 g. The supernatants were transferred to 1.2 mL glass inserts (VWR, West Chester, PA) for LC-MS/MS assay on a Shimadzu Prominence HPLC system (Columbia, MD) coupled with a 4000QTRAP mass spectrometer (AB Sciex, Framingham, MA). The GM1 were separated on an ACE Super C18 column (4.6 x 50 mm, 3 µm) (Mac-Mod Analytical, Chadds Ford) protected with a SecurityGuard Gemini C18 guard column (4 x 3 mm) (Phenomenex, Torrance, CA). The mobile phases consisted of in 2·9 mM diethylamine and 20 mM hexafluoro-2-propanol in water (solvent A) and methanol-tetrahydrofuran (97:3) (solvent B), and the flow rate was 1 mL/min. The gradient was as follows: 0 to 4 min, 85 to 100% solvent B; 4 to 6 min, 100% solvent B; 6 to 6·1 min, 100 to 85% solvent B; 6·1 to 8 min, 60% solvent B. The eluate was directed into the mass spectrometer for data acquisition from 1·8 to 4 min; elsewhere, eluate was sent to waste to minimize source contamination. The injection volume was 4 µL, and the total run-time was 8 min. The electrospray ionization (ESI) source temperature was 500 ºC; the electrospray voltage was -4500 V. The multiple reaction monitoring (MRM) transitions of *m/z* 1516·8 to 290·1, 1544·9 to 290·1, 1572·9 to 290·1, 1547·9 to 290·1 were used to detect GM1(16:0), GM1(18:0), GM1(20:0), d_3-GM1(18:0), respectively. The dwell time, declustering potential (DP), collision energy (CE), entrance potential (EP), and the collision cell exit potential (CXP) were 50 ms, -210 eV, -97 eV, -10 eV, and -10 eV, respectively, for all the MRM transitions. Data were acquired and analyzed by Analyst software (version 1.6.3).

Profiling of oligosaccharides in human plasma, CSF, urine and cat CNS samples from GM1 gangliosidosis natural history study

The cat CNS tissues (100 - 300 mg) were homogenized in water (4 mL/g wet tissue) in 2 mL Omni homogenization tubes containing 8 mm ceramic beads and processed on the Bead Ruptor 24 (Omni International, Kennesaw, GA) for two 30 second cycles at 5·65 m/s with a 45 second dwell. Human plasma, CSF, urine, cat tissue homogenate samples (50 µL) were aliquoted into 2 mL polypropylene tubes (VWR, West Chester, PA). To each tube 2-AA (30 mg/mL) and $NaBH_3CN$ (20 mg/mL) in methanol (200 µL) was added. The mixtures were vortexed for 3 min, heated at 80 °C for 1 hour, and centrifuged for 10 min at 9400 g. The supernatants were transferred to 1·2 mL glass inserts (VWR, West Chester, PA) and dried with nitrogen flow at 50 °C. The residues were partitioned between water (200 µL) and MTBE (600 µL), and aqueous phases were transfer to new 1·2 mL glass inserts for LC-MS/MS assay on a Shimadzu Prominence HPLC system (Columbia, MD) coupled with a 6500QTRAP+ mass spectrometer (AB Sciex, Framingham, MA). The oligosaccharides were separated on an ACE C18 column (4·6 x 150 mm, 3 µm) (Mac-Mod Analytical, Chadds Ford) protected with a SecurityGuard C18 guard column (4 x 3 mm) (Phenomenex, Torrance, CA). The mobile phases consisted of 0·1% formic acid in water (solvent A) and 0·1% formic acid in methanol-acetonitrile (4:1) (solvent B), and the flow rate was 1 mL/min. The gradient was as follows: 0 to 10 min, 3 to 40% solvent B; 10 to 10·1 min, 40 to 100% solvent B; 10·1 to 11 min, 100% solvent B; 11 to 11·1 min, 100 to 3% solvent B; 11·1 to 13 min, 3% solvent B. The eluate was directed into the mass spectrometer for data acquisition from 8 to 11 min; elsewhere, eluate was sent to waste to minimize source contamination. The injection volume was 2 µL, and the total run-time was 13 min. The ESI source temperature was 500 ºC; the electrospray voltage was 5500 V; the DP was 75 V; the EP and the CXP were 10 and 10 V, respectively. The collision and curtain gas were set at medium and 30, respectively. Both desolvation gas and nebulizing gas were set at 35 L/min. The CEs for MRM transitions of m/z 1032·4 to 667·3 (quantifier for 2-AA derivatized H3N2a and H3N2b) and m/z 1032·4 to 343·1 (qualifier for 2-AA derivatized H3N2a and H3N2b) were 30 and 45 eV, respectively. The dwell time was set at 50 ms for both MRM transitions. Data were acquired and analyzed by Analyst software (version 1.6.3).

Assay of β-galactosidase activity

The frozen sections (50 µm) were cut from cat cervical intumescence, frontal cortex, lumbar intumescence, and occipital cortex issue and homogenized manually in 50 mM citrate phosphate buffer, pH 4·4 (50 mM citric acid, 50 mM disodium hydrogen phosphate, 10 mM sodium chloride) containing 0·1% TritonX and 0·05% bovine serum albumin, followed by 2 freeze-thaw cycles and centrifugation at 15,700 g for 5 minutes at 4 °C. The activity of β-galactosidase was measured using synthetic fluorogenic substrate 4MU-β-D-galactoside as previously described.[1] Specific activity normalized to protein concentration by the Lowry method was expressed as nmol 4MU/mg protein/hr.

STRUCTURE IDENTIFICATION OF PENTASACCHARIDES

Experimental Details

Liquid chromatography-enhanced product ion scan (LC-EPI) of 2-AA derivatized H3N2a and H3N2b
The HPLC condition was same as that used to profile oligosaccharides in human plasma, CSF, urine and cat CNS samples. The ESI source temperature was 500 ºC; the electrospray voltages for both 2-AA derivatized H3N2a and H3N2b ions at *m/z* 1032·4 ($[M+H]^+$), 1054·4 ($[M+Na]^+$), 1030·4 ($[M-H]^-$) were 5500, 5500, -4500V, respectively; the DP were 80, 80, -80 V for $[M+H]^+$, $[M+Na]^+$, $[M-H]^-$ ions of both 2-AA derivatized H3N2a and H3N2b, respectively; the mass scan range was *m/z* 50-1400; scan speed was 10000 u/s; and dynamic fill time was used; the CE for EPI scan of $[M+H]^+$, $[M+Na]^+$, $[M-H]^-$ ions of both 2-AA derivatized H3N2a and H3N2b were 40, 80, -90 eV, respectively. The collision and curtain gas were set at high and 30, respectively. Both desolvation gas and nebulizing gas were set at 35 L/min. Data were acquired and analyzed by Analyst software (version 1.6.3).

Enzymatic degradation of 2-AA derivatized H3N2a and H3N2b
The HPLC fractions of 2-AA derivatized H3N2a and H3N2b were dissolved in 50 μL of β(1-4)-galactosidase (0·2 U/mL) in ammonium acetate buffer (0·05 M, pH 6·0) and incubated at 37 °C for 3 hours. The 2 μL of mixture was diluted with 18 μL of water followed by LC-MS/MS assay. The rest mixture was dried with nitrogen flow at 50 °C, and the residue was dissolved in 50 μL of β-N-acetylhexosaminase (4 U/mL) in ammonium acetate buffer (0·05 M, pH 6·0) followed by incubation at 37 °C for 16 hours. The 2 μL of mixture was diluted with 18 μL of water followed by LC-MS/MS assay. The rest mixture was dried with nitrogen flow at 50 °C, and the residue was dissolved in 50 μL of α(1-2,3,6)-mannosidase (15 U/mL) and zinc chloride (1 mM) in ammonium acetate buffer (0·05 M, pH 4·5) followed by incubation at 37 °C for 3 hours. The 2 μL of mixture was diluted with 18 μL of water followed by LC-MS/MS assay. The rest mixture was dried with nitrogen flow at 50 °C, and the residue was dissolved in 50 μL of β-mannosidase (10 U/mL) in ammonium acetate buffer (0·1 M, pH 4·0) followed by incubation at 37 °C for 3 hours. The 2 μL of mixture was diluted with 18 μL of water followed by LC-MS/MS assay. The 2-AA-N-acetylglucosamine was prepared from reductive amination of N-acetylglucosamine in aqueous solution (10 μg/mL, 50 μL) with 2-AA and $NaBH_3CN$ as described in profiling of oligosaccharides in human plasma, CSF, urine and cat CNS samples from GM1 gangliosidosis natural history study. LC-EPI scans of enzymatic degradation products were performed on a Shimadzu Prominence HPLC system coupled with the 6500QTRAP+ mass spectrometer. The ACE C18 column (4·6 x 150 mm, 3 μm) protected with a SecurityGuard C18 guard column (4 x 3 mm) was used to separate the degradation products from enzymatic reaction matrixes. The mobile phases consisted of 0·1% formic acid in water (solvent A) and 0·1% formic acid in methanol-acetonitrile (4:1) (solvent B), and the flow rate was 1 mL/min. The gradient was as follows: 0 to 8·4 min, 5 to 24% solvent B; 8·4 to 8·5 min, 24 to 100% solvent B; 8·5 to 10.5 min, 100% solvent B; 10·5 to 10·6 min, 100 to 5% solvent B; 10·6 to 12 min, 5% solvent B. The eluate was directed into the mass spectrometer for data acquisition from 4 to 10 min; elsewhere, eluate was sent to waste to minimize source contamination. The injection volume was 1 μL for all the degradation products, and the total run-time was 12 min. The ESI source temperature was 500 ºC; the electrospray voltage was 5500 V; the DP was 75 V; the mass scan range was *m/z* 50 - 900; scan speed was 10000 u/s; and dynamic fill time was used; the CE for EPI scan of $[M+H]^+$ ions of both 2-AA derivatized H3N2a and H3N2b digested with 1) β1,4 galactosidase (*m/z* 870.3); 2) β1,4 galactosidase, β-N-acetylglucosaminidase (*m/z* 667.2); 3) β1,4 galactosidase, β-N-acetylglucosaminidase, α-1-2,3,6-mannosidase (*m/z* 505.2); 4) β1,4 galactosidase, β-N-acetylglucosaminidase, α-1-2,3,6-mannosidase, and β-mannosidase (*m/z* 343.1), were 35, 35, 35, 25 eV, respectively. The collision and curtain gas were set at high and 30, respectively. Both desolvation gas and nebulizing gas were set at 35 L/min. Data were acquired and analyzed by Analyst software (version 1.6.3).

$NaIO_4$ oxidation and $NaBH_4$ reduction of 2-AA derivatized H3N2a and H3N2b
The HPLC fractions of 2-AA derivatized H3N2a and H3N2b were dissolved in 50 μL of $NaIO_4$ (40 mM) in ammonium acetate buffer (0·1 M, pH 6·5), and the reaction mixtures were left stand at 4 °C in the dark for 3 days. The oxidation was quenched by addition of 2 μL of ethylene glycol followed by standing at room temperature for 1 hour. To this reaction mixture was added 100 μL of $NaBH_4$ (10 mg/mL) in ammonium hydroxide (2 M) solution, the final reaction mixture was left stand at room temperature for 1 hour followed by quenching with 4·3 μL of acetic acid. The final mixture was directly submitted to LC-MS/MS assay.

LC-EPI scans of $NaIO_4$ and $NaBH_4$ treated products were performed on a Shimadzu Prominence HPLC system (Columbia, MD) coupled with the 6500QTRAP+ mass spectrometer (AB Sciex, Framingham, MA). The ACE C18 column (4·6 x 150 mm, 3 μm) protected with a SecurityGuard C18 guard column (4 x 3 mm) was used to separate the degradation products from enzymatic reaction matrixes. The mobile phases consisted of 0.1% formic acid in water (solvent A) and 0.1% formic acid in methanol-acetonitrile (4:1) (solvent B), and the flow rate was 1 mL/min. The

gradient was as follows: 0 to 8·4 min, 5 to 36% solvent B; 8·4 to 8·5 min, 36 to 100% solvent B; 8·5 to 10·5 min, 100% solvent B; 10·5 to 10·6 min, 100 to 5% solvent B; 10·6 to 12 min, 5% solvent B. The eluate was directed into the mass spectrometer for data acquisition from 4 to 10 min; elsewhere, eluate was sent to waste to minimize source contamination. The injection volume was 20 μL for all the degradation products of 2-AA derivatized H3N2a and H3N2b, and the total run-time was 12 min. The ESI source temperature was 500 ºC; the electrospray voltages were 5500 and -4500V for positive and negative modes, respectively; the DP was 75 and -75 V for positive and negative modes, respectively; the mass scan range was *m/z* 50 - 1000; scan speed was 10000 u/s; and dynamic fill time was used; the CEs for EPI scans of ions at *m/z* 948·4 (degradation product of 2-AA derivatized H3N2a, $[M+H]^+$), *m/z* 976·4 (degradation product of 2-AA derivatized H3N2b, $[M-H]^+$), *m/z* 946·4 (degradation product of 2-AA derivatized H3N2a, $[M-H]^-$), *m/z* 974·4 (degradation product of 2-AA derivatized H3N2b, $[M-H]^-$) were 50 50, -80, and -80 eV, respectively. The collision and curtain gas were set at high and 30, respectively. Both desolvation gas and nebulizing gas were set at 35 L/min. Data were acquired and analyzed by Analyst software (version 1.6.3).

Results

The 2-AA derivatized H3N2a and H3N2b can be detected as $[M+H]^+$, $[M-H]^-$, and $[M+Na]^+$ ions, which generated unique product ions in collision-induced dissociation (CID). The Y_1 - Y_4 ions generated from glycosidic bond cleavages of $[M+H]^+$ (*m/z* 343, 505, 667, 870) (**Fig. 2b**), $[M+Na]^+$ ions (*m/z* 365, 527, 689, 892) (**Fig. S2a**, **S3a**, and **S4b**), and $[M-H]^-$ (*m/z* 341, 503, 665, 868) (**Fig. S3c** and **S3d**) indicate that the sequences of both oligosaccharides are ^{5}Hexose-^{4}N-acetylhexosamine-^{3}Hexose-^{2}Hexose-^{1}N-acetylhexosamine. The cross-ring cleavage of $^{3,5}A_2$ (*m/z* 259) in $[M+Na]^+$ ions of 2-AA-H3N2a and 2-AA-H3N2b suggest that ^{5}Hexose-^{4}N-acetylhexosamine is connected by 1,4-linkage (**Fig. S2a**). Oxidation with sodium periodate ($NaIO_4$) can selectively cleave adjacent hydroxyl groups to the aldehydes that are converted into more stable alcohols by sodium borohydride ($NaBH_4$) reduction. The CID of $[M-H]^-$ ion of product from $NaIO_4$ oxidation - $NaBH_4$ reduction of 2-AA-H3N2a showed opening of pyranose ring without loss of carbon in ^{3}Hexose (Y_3 ion at *m/z* 609), losses of CHOH from ^{2}Hexose (Y_2 ion at *m/z* 445) and CH_2OH from ^{1}N-acetylhexosamine (Y_1 ion at *m/z* 311), suggesting that ^{4}N-acetylhexosamine-^{3}Hexose, ^{3}Hexose-^{2}Hexose and ^{2}Hexose-^{1}N-acetylhexosamine are connected by 1,2 (or 1,4)-, 1,6- and 1,4-linkages, respectively (**Fig. S2b** and **S4a**). Fragmentation of $[M-H]^-$ ion of $NaIO_4$ - $NaBH_4$ treated 2-AA-H3N2b demonstrated open of pyranose ring without loss of carbon in ^{3}Hexose (Y_3 ion at *m/z* 637), intact ^{2}Hexose (Y_2 ion at *m/z* 473), and loss of CH_2OH from ^{1}N-acetylhexosamine (Y_1 ion at *m/z* 311), suggesting that ^{4}N-acetylhexosamine-^{3}Hexose, ^{3}Hexose-^{2}Hexose and ^{2}Hexose-^{1}N-acetylhexosamine are connected by 1,2 (or 1,4)-, 1,3- and 1,4-linkages, respectively (**Fig. S2b** and **S4b**). The product ion (D ion) at *m/z* 410 from CID of $[M+H]^+$ ions of $NaIO_4$ - $NaBH_4$ treated 2-AA-H3N2a and 2-AA-H3N2b suggests that their ^{4}N-acetylhexosamine-^{3}Hexose is connected by 1,2-linkage (**Fig. S2c**, **S4c**, and **S4d**). The sequential loss of galactose, N-acetylglucosamine, mannose, mannose from 2-AA-H3N2a and 2-AA-H3N2b was observed following the stepwise digestion with β1,4-galactosidase, β-N-acetylglucosaminidase, α-1-2,3,6-mannosidase, and β-mannosidase (**Fig. S2d** and **S5**). The reducing terminus of both 2-AA-H3N2a and 2-AA-H3N2b is 2-AA-N-acetylglucosamine that was confirmed with a standard compound. The H3N2a and H3N2b were identified as O-β-D-galactopyranosyl-(1→4)-O-(2-acetamido-2-deoxy-β-D-glucopyranosyl)-(1→2)-O-α-D-mannopyranosyl-(1→6)-O-β-D-mannopyranosyl-(1→4)-2-acetamido-2-deoxy-α,β-D-glucopyranose and O-β-D-galactopyranosyl-(1→4)-O-(2-acetamido-2-deoxy-β-D-glucopyranosyl)-(1→2)-O-α-D-mannopyranosyl-(1→3)-O-β-D-mannopyranosyl-(1→4)-2-acetamido-2-deoxy-α,β-D-glucopyranose, respectively. They are moieties of complex N-glycan.

SYNTHESIS OF H3N2b AND d_6-H3N2b

Benzyl-3,4,6-O-tri-benzyl-α-D-mannopyranosyl-(1→3)-2-O-benzyl-4,6-O-benzylidene-β-D-mannopyranosyl-(1→4)-3,6-O-di-benzyl-2-deoxy-phthalimido-β-D-glucopyranoside (2)

Compound **1**[2] (10·68 g, 7·66 mmol, 1 eq) was dissolved in methanol/dichloromethane solvent mixture (3:2, 76 mL) followed by dropwise addition of sodium methoxide in methanol (0·5 M, 1·5 mL, 0·766 mmol, 0·1 eq). The reaction mixture was stirred overnight, quenched with ammonium chloride (0·65 g), sonicated for 5 min, and concentrated. The residue was purified by chromatography on a silica gel column (hexanes/ethyl acetate, 4:1→3:1 →2:1 → 1:1) to give **2** (9·18 g, 88·5%). ESI-MS: $[M + NH_4]^+$, calculated for $C_{82}H_{85}N_2O_{17}^+$: *m/z* 1369·5843; found: *m/z* 1369·5812. ^{1}H NMR (CDCl3, 400 MHz): δ 7·71-7·74 (m, 2 H), 7·56-7·61 (m, 4 H), 7·33-7·51 (m, 28 H), 7·15-7·24 (m, 5 H), 7·06-7·08 (m, 2 H), 6·96-7·00 (m, 3 H), 5·78 (brs, 1 H), 5·65 (s, 1 H), 5·49 (d, J = 0·8 Hz, 1 H), 5·29 (d, J = 7·8 Hz, 1 H), 4·92-5·06 (m, 5 H), 4·84 (d, J = 11·2 Hz, 1 H), 4·80 (d, J = 11·9 Hz, 1 H), 4·77 (d, J = 11·8 Hz, 1 H), 4·75 (d, J = 8·9 Hz, 1 H), 4·51-4·67 (m, 6 H), 4·41 (t, J = 4·4 Hz, 2 H), 4·33 (dd, J = 10·4, 4·7 Hz, 1 H), 3·88-4·24 (m, 8 H), 3·80 (t, J = 10·5 Hz, 2 H), 3·58-3·69 (m, 5 H); ^{13}C NMR (CDCl3, 100 MHz): δ 167·9, 138·9, 138·7, 138·5, 138·3, 138·0, 137·9, 137·5, 137·3, 133·8, 131·8, 128·9, 128·8, 128·6, 128·5, 128·4, 128·3, 128·2, 128·1, 128·0, 127·9,

127·8, 127·1, 126·2, 123·3, 101·7, 101·2, 98·9, 97·6, 79·1, 78·8, 78·4, 78·1, 77·6, 75·7, 75·5, 75·2, 75·0, 74·6, 74·4, 73·7, 73·6, 72·5, 71·7, 70·9, 69·3, 68·5, 68·3, 67·1, 55·9.

Benzyl-O-(2,3,4,6-tetra-O-acetyl-β-D-galactopyranosyl)-(1→4)-O-(3,6-di-O-acetyl-2-deoxy-2-phthalimido-β-D-glucopyranosyl)-(1→2)-O-(3,4,6-tri-O-benzyl-α-D-mannopyranosyl)-(1→3)-O-(6-O-acetyl-2,4-di-O-benzyl-β-D-mannopyranosyl)-(1→4)-3,6-O-di-benzyl-2-deoxy-phthalimido-β-D-glucopyranoside (4)

A mixture of compound **2** (8·1 g, 6 mmol, 1 eq) and lactosamine bromide **3**[3] (19·2 g, 24 mmol, 4 eq) was azeotropically dried with toluene (2 x 100 mL), dissolve in dichoromethane (40 mL) and hexane (100 mL), evaporated, and then on high vacuum for 0·5 h. Freshly activated 4 Å molecular sieves (40 g) and dichoromethane (52 mL) were added, and the mixture was stirred for 0·5 hour under a nitrogen atmosphere in the dark. The mixture was cooled to -60 °C, and 2,6-lutidine (2·79 mL, 24 mmol, 4 eq) was added. Silver trifluoromethanesulfonate (6·17 g, 24 mmol, 4 eq) was azeotropically dried with toluene (2 x 100 mL), then on high vacuum for 2 h, and dissolved in toluene (52 mL). The silver trifluoromethanesulfonate in toluene was added dropwise over 20 min to the mixture of compounds **2** and **3** and molecular sieves, and the final mixture was stirred and allowed to warm up to room temperature overnight. The reaction was quenched with saturated sodium thiosulfate solution. The mixture was diluted with dichloromethane and filtered through Celite. The organic phase is dried with magnesium sulfate, filtered, and concentrated in vacuum. The residue was purified by chromatography on a silica gel column (hexanes/ethyl acetate, 4:1→2:1 → 1:1) to give **4** (12·79 g, 92%). ESI-MS: $[M + NH_4]^+$, calculated for $C_{114}H_{120}N_3O_{34}^+$, *m/z* 2074·7748; found: *m/z* 2074·7707. ^{1}H NMR (CDCl3, 400 MHz): δ 7·70-7·73 (m, 2 H), 7·46-7·67 (m, 11 H), 7·22-7·41 (m, 20 H), 7·12-7·21 (m, 5 H), 7·01-7·12 (m, 5 H), 6·91-6·98 (m, 2 H), 6·82-6·92 (m, 3 H), 5·66 (t, J = 9·6 Hz, 1 H), 5·46 (s, 1 H), 5·41 (s, 1 H), 5·24-5·32 (m, 1 H), 4·99-5·23 (m, 4 H), 4·65-4·97 (m, 7 H), 4·41-4·61 (m, 5 H), 4·21-4·41 (m, 5 H), 3·74-4·21 (m, 14 H), 3·36-3·72 (m, 9 H), 2·78 (m, 2H), 2·17 (s, 3H), 2·15 (s, 3H), 2·08 (s, 3H), 2·02 (s, 3H), 1·97 (s, 3H); ^{13}C NMR (CDCl3, 100 MHz): δ 169·9, 169·8, 169·7, 169·6, 169·4, 168·7, 167·5, 167·1, 138·3, 138·2, 137·9, 137·8, 137·3, 137·1, 131·4, 131·1, 131·0, 130·5, 128·8, 128·6, 128·5, 128·3, 128·9, 127·9,127·8, 127·7, 127·6,127·5,127·5, 127·4, 127·3, 127·2, 127·2, 127·1, 126·5, 124·9, 123·5, 122·8, 101·8, 100·8, 100·4, 96·9, 94·7, 78·4, 77·7, 77·5, 76·3, 76·0, 74·5, 74·4, 74·1, 74·0, 73·5, 73·0, 72·4, 71·5, 71·3, 71·2, 70·8, 70·3, 70·1, 70·0, 69·9, 68·8, 68·2, 67·6, 66·3, 65·9, 60·9, 60·4, 55·2, 54·1, 21·1, 21·0, 20·2, 20·2, 20·1, 20·0.

O-β-D-galactopyranosyl-(1→4)-O-(2-acetamido-2-deoxy-β-D-glucopyranosyl)-(1→2)-O-α-D-mannopyranosyl-(1→3)-O-β-D-mannopyranosyl-(1→4)-2-acetamido-2-deoxy-α,β-D-glucopyranose (H3N2b)

A mixture of **4** (7·63 g, 3·71 mmol), n-butanol (26 mL), and ethylenediamine (13 mL, 196 mmol, 53 eq) was heated at 90 °C for overnight. The mixture was evaporated in vacuum, and the residue was dissolved in methanol (15 mL) and co-evaporated with toluene (3 x 100 mL), and then on high vacuum for 2 days. The residue was then dissolved in pyridine (19·6 mL, 244 mmol, 66 eq) and acetic anhydride (19·6 mL, 196 mmol, 53 eq) was added and the mixture stirred overnight. The reaction was then concentrated under reduced pressure and the residue co-evaporated with toluene (2x10 mL) and dissolved in tetrahydrofuran (30 mL). Liquid ammonia (300 mL) was condensed at –78° C into a 3-neck flask (1000 mL) with solid sodium (5 g, 219 mmol, 59 eq) equipped with mechanic stir and Dewar-type condenser. The resulting deep blue solution was stirred for 30 min. A solution of product from last step in tetrahydrofuran was added, and the reaction mixture was stirred for an additional 2 hours at -78 °C. The reaction was quenched with methanol (50 mL). The reaction vessel was subsequently removed from its cooling bath and warmed to 25° C, and the ammonia was evaporated overnight. The mixture was dissolved in water (100 mL) and neutralized with 12N hydrochloride. The organic solvent in the mixture was removed by rotavapor. The aqueous solution of crude H3N2b was washed with tetrahydrofuran-ethyl acetate (2:1) (2 x 150 mL) and desalted by chromatography on a short charcoal column (water/acetonitrile, 1:0→3:2). The pure H3N2b (0·96 g, 28·4% overall yield over 3 steps) that is an anomeric mixture was obtained as white solid by isolation on a Hypercarb porous graphitic carbon HPLC column (4·6 x 150 mm, 3 μm) (Thermo Scientific, Waltham, MA) protected with a SecurityGuard C18 guard column (4 x 3 mm). The mobile phases consisted of 0·1% acetic acid in water (solvent A) and acetonitrile (solvent B), and the flow rate was 1 mL/min· The gradient was as follows: 0 to 15 min, 5 to 8% solvent B; 15 to 15·1 min, 8 to 10% solvent B; 15·1 to 18 min, 10% solvent B; 18 to 18·1 min, 10 to 95% solvent B; 18·1 to 21 min, 95% solvent B; 21 to 21·1 min, 95 to 5 % solvent B; 21·1 to 25 min, 5 % solvent B. ESI-MS: $[M + H]^+$, calculated for $C_{34}H_{59}N_2O_{26}^+$, *m/z* 911·3351; found: *m/z* 911·3327. $[M + Na]^+$, calculated for $C_{34}H_{58}N_2O_{26}Na^+$, *m/z* 933·3170; found: *m/z* 933·3145. ^{1}H NMR (D_2O, 600 MHz) δ 5·20 (d, J = 3 Hz, 0·64 H), 5·13 (s, 1H), 4·71-4·75 (m, 1 H), 4·58 (d, J = 7·2 Hz, 1H), 4·47 (d, J = 7·8 Hz, 1H), 4·25 (dd, J = 3Hz, 6·6 Hz, 1 H), 4·20 (s, br, 1 H), 3·98 (d, J = 10·8 Hz, 1H), 3·89-4·96 (m, 6H), 3·83-4·96 (m, 2H), 3·46-3·82 (m, 20 H), 2·06 (s, 3H), 2·05 (s, 3H)· ^{13}C NMR (D_2O, 150 MHz): 177·3, 177·0, 105·5, 102·6, 102·1, 102·1, 97·5, 93·1, 83·0, 82·0, 81·6, 81·1, 79·0, 78·7, 77·9, 77·3, 77·2, 76·1, 75·1, 74·9, 74·5, 73·5, 72·9, 72·9, 72·7, 72·0, 71·8, 71·1, 69·9, 68·5, 64·3, 63·6, 63·4, 62·7, 62·6, 62·6, 58·7, 57·4, 56·2, 24·9, 24·8, 24·5.

O-β-D-galactopyranosyl-(1→4)-O-(2-d_3-acetamido-2-deoxy-β-D-glucopyranosyl)-(1→2)-O-α-D-mannopyranosyl-(1→3)-O-β-D-mannopyranosyl-(1→4)-2-d_3-acetamido-2-deoxy-α,β-D-glucopyranose (d_6-H3N2b)

The d_6-H3N2b (0·27 g, 20·4% overall yield over 3 steps) that is an anomeric mixture was prepared as white solid from **4** (2·96 g, 1·44 mmol) by reactions with: 1) n-butanol (10 mL), and ethylenediamine (5·1 mL, 76·3 mmol, 53 eq); 2) pyridine (7·6 mL, 95 mmol, 66 eq) and d_6-acetic anhydride (7·6 mL, 76·3 mmol, 53 eq); 3) liquid ammonia (120 mL) and sodium (1·95 g, 85 mmol, 59 eq) according to the procedures that was described for the preparation of H3N2b. ESI-MS: $[M+H]^+$, calculated for $C_{34}H_{53}D_6N_2O_{26}^+$, *m/z* 917·3727; found: *m/z* 917·3751. $[M+Na]^+$, calculated for $C_{34}H_{52}D_6N_2O_{26}Na^+$, *m/z* 939·3547; found: *m/z* 939·3572. ^{1}H NMR (D_2O, 600 MHz) δ 5·20 (d, J = 3 Hz, 0·64H), 5·13 (s, 1H), 4·71-4·75 (m, 1 H), 4·57 (d, J = 7·2 Hz, 1H), 4·46 (d, J = 7·8 Hz, 1H), 4·24 (dd, J = 3Hz, 6·6 Hz, 1 H), 4·19 (s, br, 1 H), 3·97 (d, J = 10·8 Hz, 1H), 3·89-4·96 (m, 6H), 3·83-4·96 (m, 2H), 3·46-3·82 (m, 20 H)· ^{13}C NMR (D_2O, 150 MHz) δ 177·3, 177·1, 105·5, 102·6, 102·1, 102·0, 97·5, 93·1, 83·0, 82·0, 81·6, 81·0, 79·0, 78·7, 77·9, 77·3, 77·2, 76·1, 75·6, 75·1, 74·9, 74·5, 73·5, 72·9, 72·6, 72·0, 71·8, 71·1, 69·9, 68·5, 64·3, 63·6, 63·4, 62·7, 62·6, 62·5, 58·6, 57·4, 56·2.

CONFIRMATION OF H3N2B STRUCTURE

The endogenous and synthetic H3N2b were derivatized as described in profiling of oligosaccharides in human plasma, CSF, urine and cat CNS samples from GM1 gangliosidosis natural history study, and chromatographic separation was performed on ACE C18 column (150 × 4·6 mm, 3 μm) protected with a SecurityGuard C18 guard column (4 x 3 mm) using a Shimadzu Prominence HPLC system (Columbia, MD). The mobile phases consisted of 0·1% formic acid in water (solvent A) and 0·1% formic acid in methanol-acetonitrile (4:1) (solvent B), and the flow rate was 1 mL/min. The gradient was as follows: 0 to 20 min, 10 to 30% solvent B; 20 to 20·1 min, 30 to 100% solvent B; 20·1 to 22 min, 100 solvent B; 22 to 22·1 min, 100 to 10% solvent B; 22·1 to 24 min, 10 solvent B. The eluate was directed into the mass spectrometer for data acquisition from 5.0 to 22 min; elsewhere, eluate was sent to waste to minimize source contamination. The injection volume was 2 μL, and the total run-time was 24 min. The HPLC system was coupled to a Q-Exactive Orbitrap MS (Thermo Fisher Scientific, Waltham, MA) operating with a heated electrospray interface (HESI-II) in ESI. The vaporizer temperature, the capillary temperature, spray voltage, sheath gas flow rate, auxiliary gas flow rate, ion sweep gas pressure, and S-lens RF level were set to 300 °C, 270 °C, 3·5kV, 60, 30, 2, and 55, respectively. The parallel reaction monitoring scan of *m/z* 1032·4 was acquired at a resolution of 70,000 and normalized collision energy of 30% in positive ion modes. Ion accumulation was set at $3·0 \times 10^6$ of Automatic Gain Control (AGC) and a maximum injection time of 100 ms. The analyses were performed without lock mass. Data were processed using Xcalibur™ version 2.2.1 (Thermo Fisher Scientific, Waltham, MA).

VALIDATION OF METHODS FOR H3N2b IN HUMAN URINE, PLASMA, AND CSF

Experimental Details

Stock solution preparation

The stock solutions of H3N2b (1 mg/mL) and d_6-H3N2b (1 mg/mL) were prepared in water. The internal standard working solution (1 μg/mL of d_6-H3N2b) for human urine, plasma, and CSF was prepared in methanol-water (4:1).

Standard curve and quality control (QC) samples

Because of the endogenous presence of H3N2b in human plasma, the calibration standards for urine (10, 20, 40, 200, 1000, 2000, 5000, 10000 ng/mL), plasma (1, 2, 5, 10, 50, 100, 250, 500 ng/mL), and CSF (1, 2, 5, 10, 50, 100, 250, 500 ng/mL) were prepared by spiking the H3N2b into water and serial dilutions, and the water was used as blank. The pooled human urine, plasma, and CSF were analyzed to establish the mean concentration of endogenous H3N2b levels and used to prepare low QC (LQC), middle (MQC), high QC (HQC), and dilution QC (DQC). The LQC (endogenous level + 100 ng/mL for urine; endogenous level + 10 ng/mL for plasma, endogenous level + 10 ng/mL for CSF), MQC (endogenous level + 4000 ng/mL for urine; endogenous level + 200 ng/mL for plasma, endogenous level + 200 ng/mL for CSF), HQC (endogenous level + 8000 ng/mL for urine; endogenous level + 400 ng/mL for plasma, endogenous level + 400 ng/mL for CSF), and DQC (endogenous level + 16000 ng/mL for urine; endogenous level + 800 ng/mL for plasma; endogenous level + 800 ng/mL for CSF) were prepared. The H3N2b in the DQC samples were higher than the upper limit of quantification (ULOQ), and the DQC samples were diluted 1:4 with water, prior to extraction.

Sample preparation

For urine, standards, QCs, blank or study samples (50 μL) were aliquoted into 2 mL polypropylene tubes. To each sample 50 μL of internal standard (1 μg/mL of d_6-H3N2b in methanol-water (4:1) was added and 50 μL of methanol-

water (4:1) was used for a blank followed by addition of 200 µL of methanol. The samples were vortexed for 3 min, centrifuged for 10 min at 9400 g, and supernatant transferred and dried with nitrogen flow at 50 °C into clean 1·2 mL glass inserts. To each insert 2-AA (30 mg/mL), $NaBH_3CN$ (20 mg/mL), sodium acetate trihydrate (40 mg/mL) and boric acid (20 mg/mL) in methanol-water (4:1) (50 µL) was added. The mixtures were vortexed for 3 min, heated at 50 °C for 1 hour, and dried with nitrogen flow at 50 °C. The residues were partitioned between water (200 µL) and MTBE (600 µL), and aqueous phases were transfer to new 1·2 mL glass inserts for LC-MS/MS assay.

For plasma and CSF, standards, QCs, blank or study samples (100 µL) were aliquoted into 2 mL polypropylene tubes. To each sample 50 µL of internal standard (1 µg/mL of d_6-H3N2b in methanol-water (4:1) was added and 50 µL of methanol-water (4:1) was used for a blank followed by addition of 400 µL of methanol. The samples were vortexed for 3 min, centrifuged for 10 min at 9400 g, and supernatant transferred and dried with nitrogen flow at 50 °C into clean 1·2 mL glass inserts. To each insert 2-AA (30 mg/mL), $NaBH_3CN$ (20 mg/mL), sodium acetate trihydrate (40 mg/mL) and boric acid (20 mg/mL) in methanol-water (4:1) (50 µL) was added. The mixtures were vortexed for 3 min, heated at 50 °C for 1 hour, and dried with nitrogen flow at 50 °C. The residues were partitioned between water (200 µL) and MTBE (600 µL), and aqueous phases were transfer to new 1·2 mL glass inserts for LC-MS/MS assay.

LC-MS/MS analysis

LC–MS/MS analysis was conducted on a Shimadzu Prominence HPLC system coupled with the 6500QTRAP+ mass spectrometer. The H3N2b and d_6-H3N2b were separated on a Halo Phenyl-Hexyl (4·6 mm x 150 mm, 2·7 µm) (Mac-Mod Analytical, Chadds Ford) protected with a SecurityGuard Phenyl guard column (4 x 3 mm) (Phenomenex, Torrance, CA). The mobile phases consisted of 0·1% acetic acid in water (solvent A) and methanol-acetonitrile (1:1) (solvent B), and the flow rate was 0·8 mL/min. The gradient was as follows: 0 to 15 min, 10 to 20% solvent B; 15 to 15·1 min, 20 to 100% solvent B; 15·1 to 17 min, 100% solvent B; 17 to 17·1 min, 100 to 10% solvent B; 17·1 to 19 min, 10% solvent B. The eluate was directed into the mass spectrometer for data acquisition from 11·5 to 14·5 min. The total run-time was 19 min, and the injection volume was 5, 10, 10 µL for urine, plasma, and CSF samples, respectively. The ESI source temperature was 500 ºC; the electrospray voltage was 5500 V; the DP, EP and the CXP was 40, 10 and 10 V, respectively. The collision and curtain gas were set at medium and 30, respectively. The desolvation gas and nebulizing gas were set at 50 and 60 L/min, respectively. The $[M+2H]^{2+}$ ion of H3N2b was used to set up the MRM transitions, which showed higher sensitivity than $[M+H]^+$ ion. The CEs for MRM transitions of m/z 516·7 to 667·3 (quantifier for 2-AA derivatized H3N2b), m/z 516·7 to 343·1 (qualifier for 2-AA derivatized H3N2b), and m/z 519·7 to 670·3 (d_6-H3N2b) were 15, 15, and 15 eV, respectively. The dwell time was set at 100 ms for all the MRM transitions. Data were acquired and analyzed by Analyst software (version 1.6.3). Calibration curves were constructed by plotting the corresponding peak area ratios of analyte/internal standard versus the corresponding analyte concentrations using weighted ($1/x^2$) linear least squares regression analysis.

Validation of linearity, precision and accuracy

The linearity, precision and accuracy of assay were evaluated over three analytical runs. In the validation analytical run, a set of samples that were analyzed in one batch, including calibration standards in duplicate, a blank, a blank with internal standard, and QC samples. This set of samples were prepared and analyzed in three different batches. The replication was the repeated preparation and analysis of the same sample. The linearity response of H3N2b was assessed over 10 - 10000 ng/mL, 1 - 500 ng/mL, and 1 - 500 ng/mL, respectively for urine, plasma, and CSF. The precision and accuracy of the assay were determined at LLOQ, LQC, MQC and HQC levels. For each QC concentration, analysis was performed in six replicates on each day except for DQCs for which three replicates were prepared in the first batch. DQC samples were analyzed in three replicates. Accuracy and precision were denoted by percent relative error (%RE) and percent coefficient of variance (%CV), respectively. The accuracy and precision were required to be within ± 15% RE of the nominal concentration and ≤15% CV, respectively, for LQC, MQC, HQC, DQC samples. The accuracy and precision were required to be within ± 20% RE of the nominal concentration and ≤20% CV for LLOQ samples in the intra-batch and inter-batch assays.

Validation of selectivity and specificity

To ascertain the selectivity of the method, blank and blank with internal standard, an ULOQ calibrator without the internal standard, and six different lots of blank biological samples (human plasma, CSF, and urine) were analyzed. To evaluate the specificity, commercially available N-complex glycans, including A1F glycan, A3 glycan, NA2F glycan, NA2 glycan, which are precursors of H3N2b, were evaluated for interferences to H3N2b. For double blank, any response at the retention times of the H3N2b was to be < 20% of the response of the LLOQ, and any response at the retention time of the internal standard was to be < 5% of the mean response of the internal standard in the

calibration curve. For the ULOQ calibrator without internal standard, any response at the retention time of the internal standard was to be < 5% of the mean response of the internal standard in the calibration curve. For the blank with internal standard, any response at the retention times of the H3N2b is to be < 20% of the response of the LLOQ. For the blank biological samples, any response at the retention time of the internal standard was to be < 5% of the mean response of the internal standard in the calibration curve. The interferences to H3N2b in N-complex glycans should be < 20% of the response of the LLOQ.

Validation of stability

The long-term storage, freeze/thaw stabilities, and stabilities on the bench-top and in the autosampler were determined at the LQC and HQC concentration levels (n = 3). Long-term storage stabilities of H3N2b -80 ºC in urine, plasma, CSF were tested. Bench-top stabilities of H3N2b were evaluated in urine at room temperature, in plasma at room temperature, in CSF at room temperature and 4 ºC. Freeze/thaw stability in urine, plasma, CSF was tested by freezing the samples at -80 ºC overnight, followed by thawing to room temperature the next day. This process was repeated three times. In the autosampler, stabilities of processed urine, plasma, CSF samples at 4 ºC were tested over 3 days by injecting the first batch of the validation samples. Stock solution stability was established by quantification of samples from dilution of two stock solutions that were stored at -20 ºC and at room temperature on the bench, respectively, to the final solution (10000 ng/mL in water). The stabilities of H3N2b in the matrix of standard curve for urine, plasma, CSF were test after storage at room temperature and at -80 °C. A fresh standard curve was established each time.

Validation of carryover

Carryover was assessed by injecting a blank sample immediately after an injection of the ULOQ calibrator.

Validation Results

Linearity and parallelism

The standard curve linear ranges for urine, plasma, and CSF were 10 - 10000 ng/mL, 1 - 500 ng/mL, 1 - 500 ng/mL, respectively. The r values of standard curves for urine, plasma, and CSF were > 0·99, and the difference in slopes of standard curves between surrogate and biological matrixes were < 6·2%. The accuracies of calibrators of standard curves for urine, plasma, and CSF were within 85 - 115%.

Sensitivity

The method sensitivities were defined by the lower limits of quantification (LLOQ) which were 10 ng/mL, 1 ng/mL, 1 ng/mL for urine, plasma, and CSF, respectively. The sensitivity test showed that the intra- and inter-batch accuracies of the LLOQ samples were within ±10% relative error (RE), and the intra- and inter-batch coefficients of variation (CV) of the LLOQ samples were < 15% for urine, plasma, and CSF methods (**Table S1 - 3**).

Selectivity

The selectivity test showed that 1) the response in blank at the retention times of the H3N2b and internal standard were < 20% of the response of the LLOQ and < 5% of the mean response of the internal standard in the calibration curve, respectively; 2) the responses in the upper limit of quantification (ULOQ) calibrator without internal standard at the retention time of the internal standard were < 5% of the mean response of the internal standard in the calibration curve; 3) the responses in the blank with internal standard at the retention times of the H3N2b were < 20% of the response of the LLOQ; 4) the responses in blank biological samples at the retention time of the internal standard were < 5% of the mean response of the internal standard in the calibration curve. No interferences to H3N2b in N-complex glycans were observed in specificity test.

Accuracy and precision

The method accuracies and precisions were evaluated with quality control (QC) samples at low (LQC), middle (MQC), and high (HQC) levels, and the urine, plasma, and CSF methods showed intra- and inter-batch accuracies and precisions within ±15% RE and < 10% CV, respectively (**Table S1 - 3**).

Stability

The H3N2b was stable at room temperature in urine for 24 hr, after 3 freeze/thaw cycles, for 3 days in processed urine samples at 4 °C, and for 194 days at -80 °C. The H3N2b was stable at room temperature in plasma for 24 hr, after 3 freeze/thaw cycles, for 3 days in processed plasma samples at 4 °C, and for 158 days at -80 °C. The H3N2b was stable at room temperature in CSF for 2 hr and at 4 °C for 24 hr, after 3 freeze/thaw cycles, for 3 days in

processed CSF samples at 4 °C, and for 125 days at -80 °C. The H3N2b in stock solution was stable at room temperature for 24 hr and -20 °C for 232 days. The H3N2b in the matrix of standard curve for urine, plasma, CSF was stable at room temperature for 24 hr. The standard curve samples for urine, plasma, and CSF were stable at -80 °C for 194, 158, and 125 days, respectively. The stock solution of H3N2b was stable at -20 °C for 231 days.

Carryover

No carryovers were observed in blank samples following the ULOQ samples for urine, plasma, and CSF.

Dilution integrity

The dilution integrity was evaluated with dilution QC (DQC) samples, and accuracy (within ±10% RE) and precision (< 5% CV) were observed after 5-fold dilution of urine, plasma, and CSF samples.

REFERENCES

1. Martin DR, Cox NR, Morrison NE, et al. Mutation of the GM2 activator protein in a feline model of GM2 gangliosidosis. *Acta Neuropathol* 2005; **110**(5): 443-50.
2. Wu Z, Liu Y, Li L, et al. Decoding glycan protein interactions by a new class of asymmetric N-glycans. *Org Biomol Chem* 2017; **15**(42): 8946-51.
3. Arnarp J, Lönngren J. Synthesis of a tri-, a penta-, and a hepta-saccharide containing terminal N-acetyl-β-D-lactosaminyl residues, part of the 'complex-type' carbohydrate moiety of glycoproteins. *Journal of the Chemical Society, Perkin Transactions I* 1981: 2070-4.

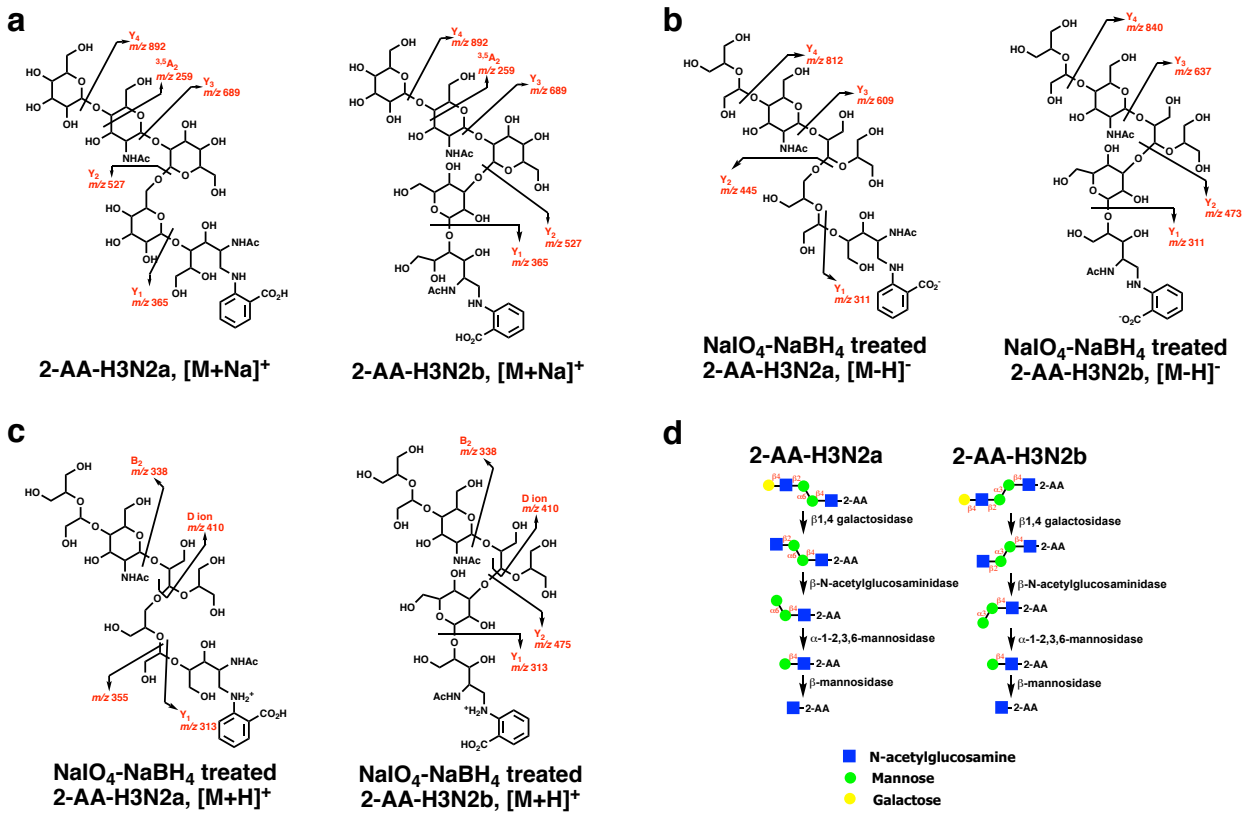

Fig. S1. Structural identification of H3N2a and H3N2b. (a) Fragmentation of $[M+Na]^+$ ions of 2-AA derivatized H3N2a and H3N2b. (b) Fragmentation of $[M-H]^-$ ions of $NaIO_4$-$NaBH_4$ treated 2-AA derivatized H3N2a and H3N2b. (c) Fragmentation of $[M+H]^+$ ions of $NaIO_4$-$NaBH_4$ treated 2-AA derivatized H3N2a and H3N2b. (d) Stepwise digestion of 2-AA derivatized H3N2a and H3N2b with β1,4 galactosidase, β-N-acetylglucosaminidase, α-1-2,3,6-mannosidase, and β-mannosidase.

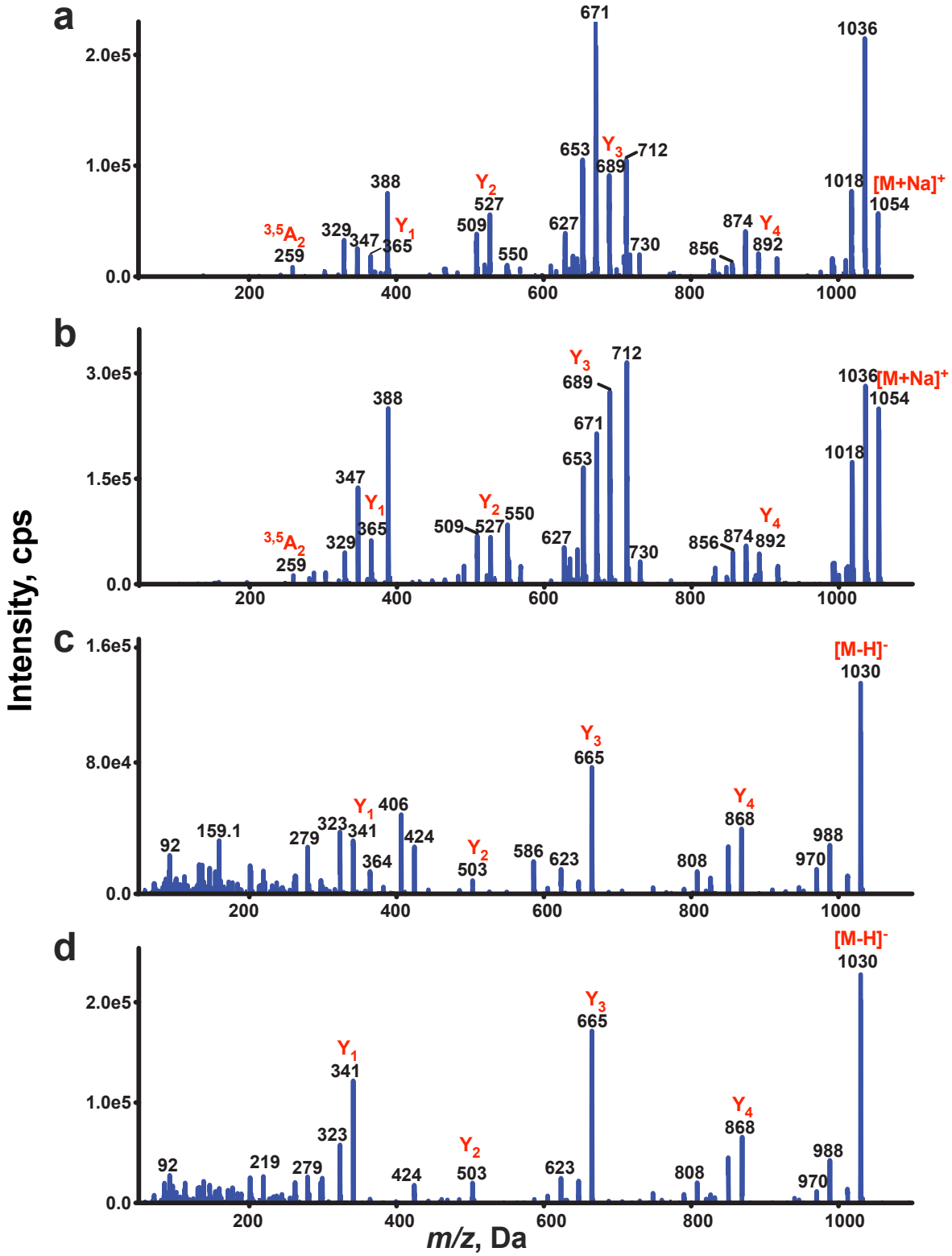

Fig. S2. EPI spectra of 2-AA derivatized H3N2a and H3N2b. (a) EPI spectrum of $[M+Na]^+$ ion of 2-AA derivatized H3N2a. (b) EPI spectrum of $[M+Na]^+$ ion of 2-AA derivatized H3N2b. (c) EPI spectrum of $[M-H]^-$ ion of 2-AA derivatized H3N2a. (B) EPI spectrum of $[M-H]^-$ ion of 2-AA derivatized H3N2b.

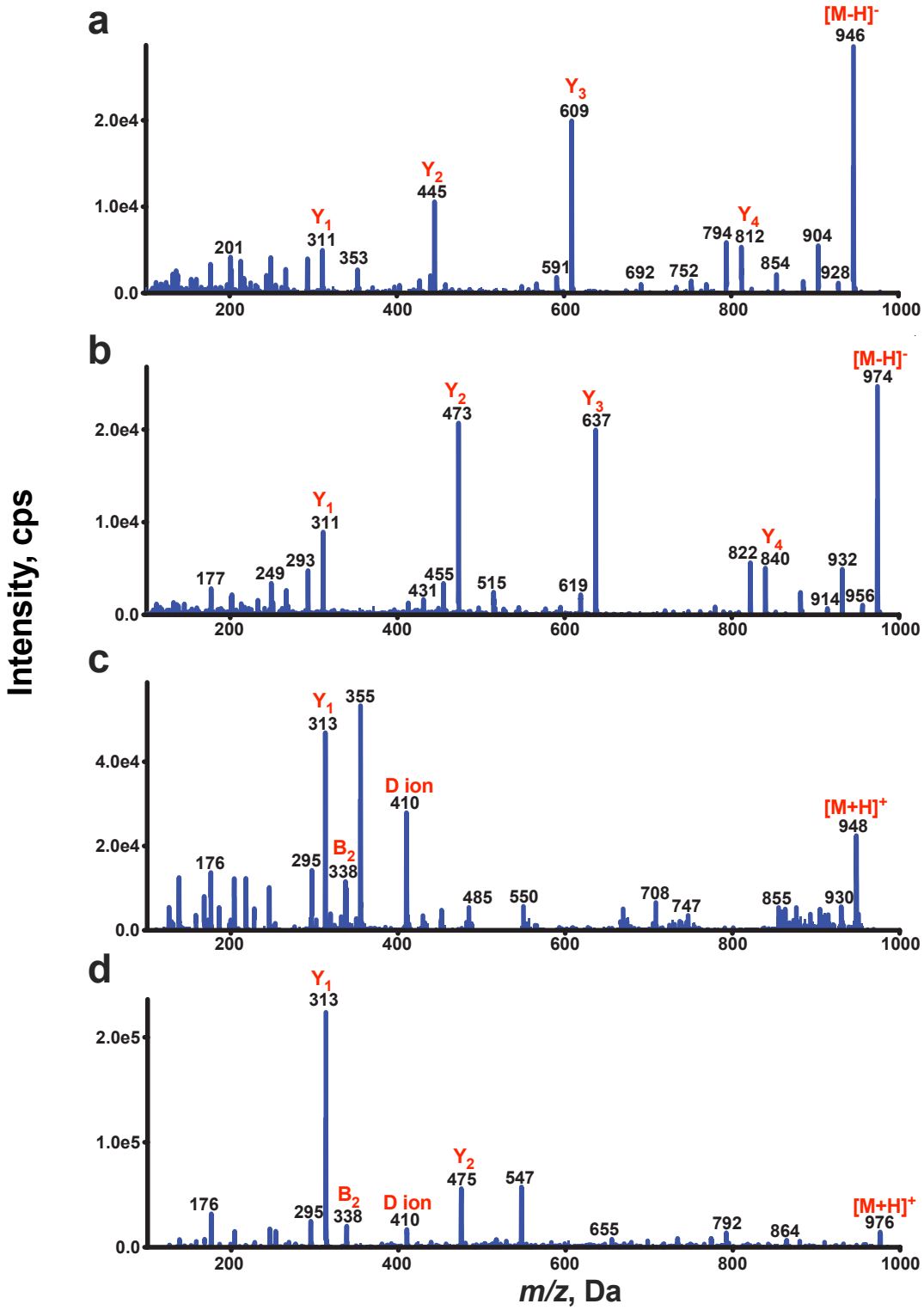

Fig. S3. EPI spectra of $NaIO_4$-$NaBH_4$ treated 2-AA derivatized H3N2a and H3N2b. (a) EPI spectrum of $[M+H]^+$ ion of $NaIO_4$-$NaBH_4$ treated 2-AA derivatized H3N2a. (b) EPI spectrum of $[M-H]^-$ ion of $NaIO_4$-$NaBH_4$ treated 2-AA derivatized H3N2a. (c) EPI spectrum of $[M+H]^+$ ion of $NaIO_4$-$NaBH_4$ treated 2-AA derivatized H3N2b. (D) EPI spectrum of $[M-H]^-$ ion of $NaIO_4$-$NaBH_4$ treated 2-AA derivatized H3N2b.

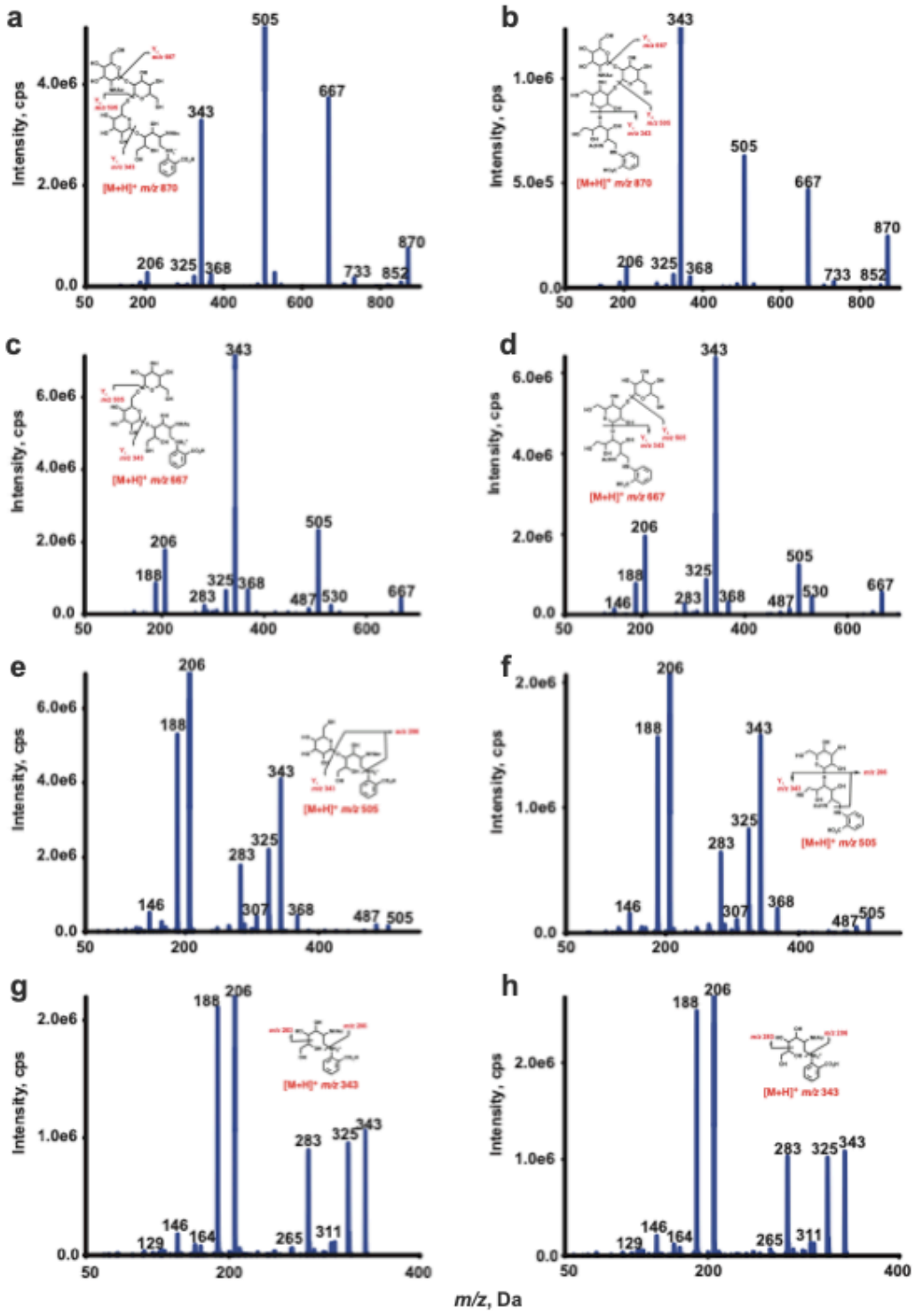

Fig. S4. EPI spectra of enzymatic degradation products of 2-AA derivatized H3N2a and H3N2b. EPI spectra of $[M+H]^+$ ion of products of 2-AA derivatized H3N2a (a) and H3N2b (b) digested with β1,4 galactosidase. EPI spectra of $[M+H]^+$ ion of products of 2-AA derivatized H3N2a (c) and H3N2b (d) digested with β1,4 galactosidase and a β-N-acetylglucosaminidase. EPI spectra of $[M+H]^+$ ion of products of 2-AA derivatized H3N2a (e) and H3N2b (f) digested with β1,4 galactosidase, β-N-acetylglucosaminidase, and α-1-2,3,6-mannosidase. EPI spectra of $[M+H]^+$ ion of products of 2-AA derivatized H3N2a (g) and H3N2b (h) digested with β1,4 galactosidase, β-N-acetylglucosaminidase, α-1-2,3,6-mannosidase, and β-mannosidase.

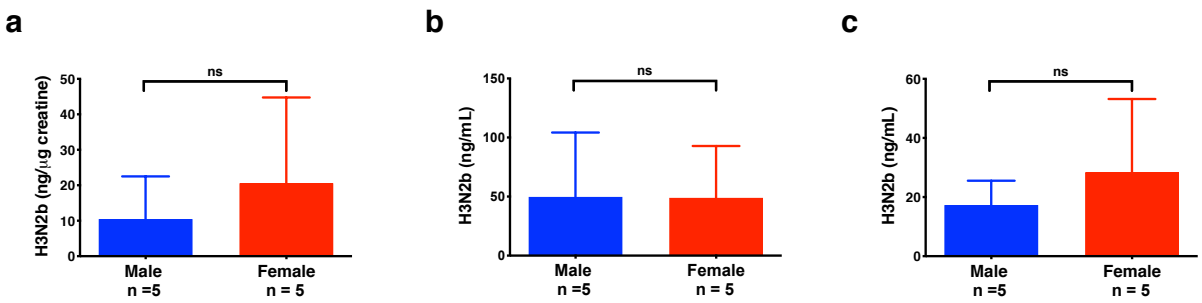

Fig. S5. Effect of gender on H3N2b in urine (a), plasma (b), CSF (c) of GM1-gangliosidosis patients. ns: not significant.

Table S1. Accuracy and precision statistics for H3N2b in urine

Run ID	QC Level	LLOQ	LQC	MQC	HQC	DQC
	Nominal concentration	10	114	4010	8010	16010
1	Intra-run mean	10·2	124	4233	8282	16233
	Intra-run SD	0·4	4·8	120	151	603
	Intra-run %CV	4·09	3·85	2·84	1·83	3·71
	Intra-run %RE	1·67	8·48	5·57	3·39	1·39
	n	6	6	6	6	3
2	Intra-run mean	10·2	117	4230	8430	
	Intra-run SD	0·2	3	178	139	
	Intra-run %CV	2·11	2·86	4·20	1·65	
	Intra-run %RE	2·33	2·63	5·49	5·24	
	n	6	6	6	6	
3	Intra-run mean	9·6	118	4342	8327	
	Intra-run SD	0·3	1	166	241	
	Intra-run %CV	2·92	1·25	3·83	2·90	
	Intra-run %RE	-3·55	3·36	8·27	3·95	
	n	6	6	6	6	
Inter-run mean		10·0	120	4268	8346	
Inter-run SD		0·4	4	157	183	
Inter-run %CV		4·01	3·73	3·67	2·20	
Inter-run %RE		0·15	4·82	6·44	4·20	
n		18	18	18	18	

Table S2. Accuracy and precision statistics for H3N2b in plasma

Run ID	QC Level	LLOQ	LQC	MQC	HQC	DQC
	Nominal concentration	1	10	200	400	800
1	Intra-run mean	0·93	10·6	196	396	827
	Intra-run SD	0·0	0·4	4·8	15	13
	Intra-run %CV	3·46	3·58	2·42	3·87	1·59
	Intra-run %RE	-6·60	5·50	-1·92	-1·08	3·38
	n	6	6	6	6	3
2	Intra-run mean	1·08	10	196	402	
	Intra-run SD	0·09	0·5	4·0	12	
	Intra-run %CV	8·31	5·29	2·03	3·10	
	Intra-run %RE	7·92	2·67	-1·83	0·46	
	n	6	6	6	6	
3	Intra-run mean	1·05	10	196	395	
	Intra-run SD	0·08	0·1	4·4	5·2	
	Intra-run %CV	7·39	1·23	2·25	1·32	
	Intra-run %RE	4·82	3·00	-2·08	-1·21	
	n	6	6	6	6	
Inter-run mean		1·02	10	196	398	
Inter-run SD		0·09	0·4	4·1	12	
Inter-run %CV		9·07	3·74	2·11	2·90	
Inter-run %RE		2·04	3·72	-1·94	-0·61	
n		18	18	18	18	

Table S3. Accuracy and precision statistics for H3N2b in CSF

Run ID	QC Level	LLOQ	LQC	MQC	HQC	DQC
	Nominal concentration	1	10	200	400	800
1	Intra-run mean	1·02	10·5	195	381	741
	Intra-run SD	0·0	0·2	2·9	6	18
	Intra-run %CV	2·09	1·68	1·49	1·59	2·38
	Intra-run %RE	2·03	4·50	-2·50	-4·83	-7·42
	n	6	6	6	6	3
2	Intra-run mean	0·95	10	187	369	
	Intra-run SD	0·10	0·1	10·1	12	
	Intra-run %CV	10·71	1·37	5·40	3·23	
	Intra-run %RE	-4·97	3·00	-6·33	-7·71	
	n	6	6	6	6	
3	Intra-run mean	0·97	10	191	376	
	Intra-run SD	0·05	0·2	2·4	4·4	
	Intra-run %CV	5·67	2·15	1·27	1·18	
	Intra-run %RE	-3·27	1·17	-4·67	-6·04	
	n	6	6	6	6	
Inter-run mean		0·98	10	191	375	
Inter-run SD		0·07	0·2	6·7	9	
Inter-run %CV		7·22	2·14	3·50	2·41	
Inter-run %RE		-2·07	2·89	-4·50	-6·19	
n		18	18	18	18	